

# Network approach integrates 3D structural and sequence data to improve protein structural comparison

Fazle E. Faisal<sup>1,5,6</sup>, Julie L. Chaney<sup>2,7</sup>, Khalique Newaz<sup>1,5,6</sup>, Jun Li<sup>3</sup>, Scott J. Emrich<sup>1</sup>, Patricia L. Clark<sup>2,4,6</sup>, and Tijana Milenković<sup>1,5,6,\*</sup>

<sup>1</sup>Department of Computer Science and Engineering, University of Notre Dame, Notre Dame, IN 46556, USA

<sup>2</sup>Department of Chemistry and Biochemistry, University of Notre Dame, Notre Dame, IN 46556, USA

<sup>3</sup>Department of Applied and Computational Mathematics and Statistics, University of Notre Dame, Notre Dame, IN 46556, USA

<sup>4</sup>Department of Chemical and Biomolecular Engineering, University of Notre Dame, Notre Dame, IN 46556, USA

<sup>5</sup>Interdisciplinary Center for Network Science and Applications, University of Notre Dame, Notre Dame, IN 46556, USA

<sup>6</sup>ECK institute for Global Health, University of Notre Dame, Notre Dame, IN 46556, USA

<sup>7</sup>Siemens Healthineers, Elkhart, IN 46516, USA

\*Corresponding author (email: tmilenko@nd.edu)

Initial protein structural comparisons were sequence-based. Since amino acids that are distant in the sequence can be close in the 3-dimensional (3D) structure, 3D contact approaches can complement sequence approaches. Traditional 3D contact approaches study 3D structures directly. Instead, 3D structures can be modeled as protein structure networks (PSNs). Then, network approaches can compare proteins by comparing their PSNs. Network approaches may improve upon traditional 3D contact approaches. We cannot use existing PSN approaches to test this, because: 1) They rely on naive measures of network topology. 2) They are not robust to PSN size. They cannot integrate 3) multiple PSN measures or 4) PSN data with sequence data, although this could help because the different data types capture complementary biological knowledge. We address these limitations by: 1) exploiting well-established graphlet measures via a new network approach, 2) introducing normalized graphlet measures to remove the bias of PSN size, 3) allowing for integrating multiple PSN measures, and 4) using ordered graphlets to combine the complementary PSN data and sequence data. We compare both synthetic networks and real-world PSNs more accurately and faster than existing network, 3D contact, or sequence approaches. Our approach finds PSN patterns that may be biochemically interesting.

## 1 Introduction

Proteins perform important cellular functions. While understanding protein function is clearly important, doing so experimentally is expensive and time-consuming<sup>1,2</sup>. Because of this, the functions of many proteins remain unknown<sup>2,3</sup>. Consequently, computational prediction of protein function has received attention. In this context, protein structural comparison (PC) aims to quantify similarity between proteins with respect to their sequence or 3-dimensional (3D) structural patterns, in order to predict functions of unannotated proteins based on functions of annotated proteins that they are similar to.

Early PC has relied on sequence analyses<sup>4,5</sup>. Due to advancements of high-throughput sequencing technologies, rich sequence data is available for many species, and thus, comprehensive sequence pattern searches are possible.

Amino acids that are distant in the linear sequence can be close in 3D structure. Thus, 3D structural analyses can reveal patterns that might not be apparent from the sequence alone<sup>6</sup>. For example, while high sequence similarity between proteins typically indicates their high structural and functional similarity<sup>3</sup>, proteins with low sequence similarity can still be structurally similar and perform similar function<sup>7,8</sup>. In this case, 3D structural approaches, unlike sequence approaches, can correctly identify structurally and thus functionally similar proteins. On the other extreme, proteins with high sequence similarity can be structurally dissimilar and perform different functions<sup>9-12</sup>. In this case, 3D structural approaches, unlike sequence approaches, can correctly identify structurally and thus functionally different proteins.

3D structural approaches can be categorized into traditional 3D contact approaches and recent network approaches. 3D contact approaches, which typically deal with 3D structural alignment, study 3D structures directly<sup>13,14</sup>. Instead, network

approaches first model 3D structures as protein structure networks (PSNs, or contact maps, in which nodes are amino acids and edges link spatially close amino acids<sup>15</sup>) and then compare proteins by comparing their PSNs. 3D contact approaches produce rigid protein alignments while comparing 3D structures<sup>16</sup>. Hence, they may not always perform well in the task of PC. Also, 3D contact approaches are typically slow. This requires alternative, more flexible and faster PC approaches. Since PSNs model spatial proximities of amino acids within the protein 3D structure, network analyses of PSNs have a potential to complement and improve upon 3D contact (as well as sequence) approaches in the task of PC.

Network analyses of 3D structures *have* received attention<sup>8,17</sup>, e.g., when comparing functionally different proteins<sup>18–20</sup>. However, these existing network approaches have limitations:

1. They rely on naive measures of network topology, which capture the global view of a network but ignore complex local interconnectivities that exist in real-world networks, including PSNs<sup>21–23</sup>. Hence, a more sensitive measure of local network topology might improve PC.
2. They can bias PC by PSN size: networks of similar topology but different sizes can be mistakenly identified as dissimilar by the existing approaches simply because of their size difference. Thus, PC strategies are needed that can avoid the PSN size bias.
3. Because different network measures quantify the same PSN topology from different perspectives<sup>17,24</sup>, and because the existing approaches rely on a single network measure, PC could be biased towards the PSN perspective captured by the given measure. Integration of different and complementary network measures could improve PC.
4. Almost all existing network approaches ignore valuable sequence information (also, the existing sequence approaches ignore valuable PSN information). Combining the complementary ideas of network and sequence measures could improve PC.

We present a new network-based PC framework that relies on principal component analysis (PCA) and that overcomes the above drawbacks of the existing approaches. Specifically:

1. We use graphlets<sup>25,26</sup>, a sensitive measure of *local* network topology, in hope to improve PC upon the existing network approaches. While graphlets have already been proven in analyses of protein-protein interaction networks<sup>27–29</sup>, here we use them in a novel application of PC. Also, we use them within our PCA framework, where none of the existing graphlet methods rely on PCA.
2. We perform graphlet normalization to address the bias of PSN size.
3. We allow for integrating different and complementary network topological measures within our framework.
4. We adopt the idea of *ordered graphlets*<sup>16</sup> to integrate the PSN amino acid interconnectivity information with sequence information, in order to improve upon network approaches alone or sequence approaches alone. While ordered graphlets are an existing idea, this idea was introduced only on up to 3-node graphlets. However, using larger graphlets can be beneficial in many real-world contexts<sup>24,27–29</sup>. Hence, we extend the existing notion of 3-node ordered graphlets both theoretically and implementation-wise to be able to deal with larger graphlets. Importantly, even when we use only the existing up to 3-node ordered graphlets, our new PCA framework already outperforms the existing approach that is based on the same ordered graphlets<sup>16</sup>. This validates the PCA framework as a whole. Using larger graphlets helps further. Additionally, we introduce a novel concept of “*long-range(K)*” *ordered graphlets* to give higher importance to amino acids that are close enough in the protein 3D structure but are at least  $K$  amino acids apart in the protein sequence than to amino acids that are close enough in the 3D structure simply because they are also close to each other in the sequence, as such longer-range interactions might help distinguish protein structures better<sup>6,30</sup>. Indeed, “*long-range(K)*” ordered graphlets further improve accuracy compared to traditional ordered graphlets. We include the implementation of the extended idea of (larger size as well as “*long-range(K)*”) ordered graphlets into our software (available upon request).

We study two network types: synthetic networks (in order to illustrate wide applicability of our approach across many domains) and real-world PSNs (in order to illustrate a specific application of our approach in the task of PC). For each network type, we analyze multiple data sets. In each data set, each network has a known label, meaning that we know that networks having the same label should be identified as similar, while networks having different labels should be identified as dissimilar. For synthetic networks, we study 21 network approaches (Fig. 1), of which nine are different versions of our proposed graphlet PCA approach and 12 are existing (non-PCA) approaches (of which four use graphlets and eight do not use graphlets). Given a data set and a network approach, we compute similarity/distance between each pair of networks. We evaluate each approach by measuring how accurately it can identify as similar networks of the same label and as dissimilar networks of different labels. We measure this by computing the area under precision-recall curve (AUPR) and area under receiver operator characteristic curve (AUROC). For real-world networks, in addition to the 21 network approaches, we also study two 3D contact approaches and a sequence approach, and we perform the same AUPR and AUROC evaluation. (These three approaches *cannot* be used on the synthetic networks.) For details, see Methods.

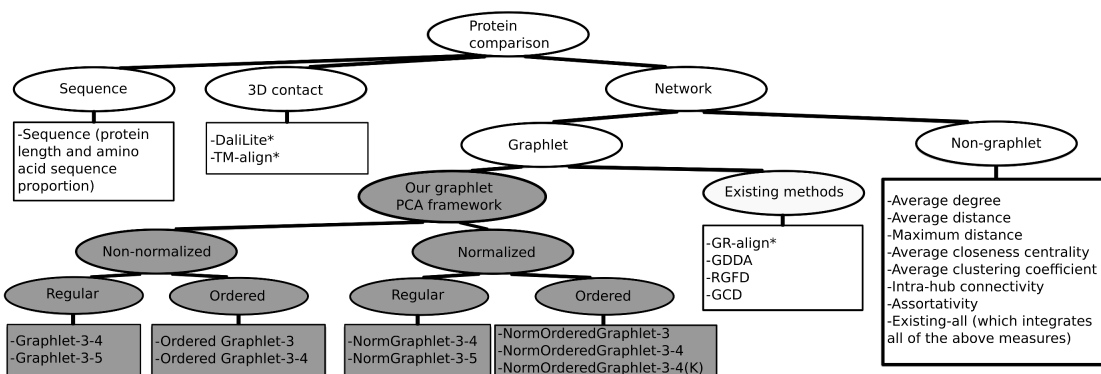


**Figure 1.** Categorization of the 24 approaches (listed in squares) that we evaluate. Different versions of our proposed graphlet PCA approach are colored in grey. Alignment-based approaches are marked with an asterisk (\*) sign; all remaining approaches are alignment-free (see Methods for details).

Our key findings are as follows. Over all data sets, our graphlet PCA approach is superior to the existing (non-PCA) graphlet and non-graphlet network approaches. We demonstrate the importance of removing the bias in PSN size, leading to a normalized version of our graphlet PCA approach that is superior to its non-normalized counterpart when controlling for network size. Combining our normalized graphlet PCA approach with sequence data via ordered graphlets results in superior accuracy compared to any network approach alone or sequence approach alone, which confirms that data integration helps. Adding the “long-range( $K$ )” constraint on the normalized ordered graphlets further improves accuracy, which additionally confirms the importance of long-range amino acid interactions. Our network approach outperforms the traditional 3D contact approaches in terms of both accuracy and running time, which confirms the power of network analyses of 3D structures. Our approach reveals PSN patterns that may be biochemically interesting. For details, see Results.

## 2 Methods

### 2.1 Data

We collect 3D atomic structures of proteins from the Protein Data Bank (PDB)<sup>31</sup>, where each protein is annotated by a label from CATH, SCOP, or both (see below). Since PDB contains multiple copies of the same or nearly identical proteins, we aim to reduce the redundancy by selecting a set of proteins from PDB such that each protein in the set is not more than 90% sequence identical to any other protein in the set. If a protein is not more than 90% sequence identical to any other protein from PDB, we immediately select the protein. If a protein is more than 90% sequence identical to one or more proteins from PDB, we select a “representative” protein from such a protein group so that the representative protein is of the highest quality (in terms of resolution) among all proteins in the group. This strategy results in the selection of 17,036 proteins. We denote this data set as *ProteinPDB*. Each protein in the data is comprised of the X, Y, and Z orthogonal Angstrom (Å) coordinates of heavy atoms (i.e., *carbon*, *nitrogen*, *oxygen*, and *sulfur*) of each amino acid within the protein. The data is available at <http://www.rcsb.org/pdb/home/home.do> for free download.

Class, Architecture, Topology, Homology (CATH) is a protein domain categorization database<sup>32,33</sup>. A protein is typically composed of one or more domains (a domain refers to a common protein structure), and the purpose of CATH is to annotate these domains. CATH’s categorization scheme is hierarchical. Its top hierarchy divides protein domains into four groups (i.e., categories or labels): *alpha* ( $\alpha$ ), *beta* ( $\beta$ ), *alpha/beta* ( $\alpha/\beta$ ), and *few secondary structures*. Only for few secondary structures, none of the domains in ProteinPDB belong to this category, and so we remove few secondary structures from further consideration. Each of the remaining three top-level CATH categories has deeper-level subcategories, which we also consider, per our discussion below.

Structural Classification of Proteins (SCOP)<sup>34</sup> is another protein domain categorization database whose categorization scheme is also hierarchical. SCOP’s top hierarchy divides protein domains into 11 groups: *alpha*, *beta*, *alpha/beta*, *alpha plus beta* ( $\alpha+\beta$ ), *coiled coil*, *membrane*, *multi-domain*, *small*, *low resolution*, *peptide*, and *designed*. Only for small, low resolution, peptide, or designed, none of the domains in ProteinPDB belong to these categories, and so we remove these four categories from further consideration. Each of the remaining top-level SCOP categories has deeper-level subcategories, which we also consider, per our discussion below.

## 2.2 Forming networks

We evaluate the considered approaches in the task of PC on: 1) synthetic networks, i.e., on artificially generated networks for which we know the topology-based ground truth categorization, and 2) real-world PSNs, for which we know CATH or SCOP label-based categorizations that we hypothesize correlate well with the PSNs' topology-based characteristics.

**Synthetic networks.** We generate synthetic networks by using different network models. A good approach should identify networks from the same network model (i.e., with the same label) as similar, and it should identify networks from different models (i.e., having different labels) as dissimilar. Specifically, we use three well-established network models: *Erdős-Rényi random graphs (ER)*, *geometric random graphs (GEO)*, and *scale-free random graphs (SF)*<sup>21,23</sup>. We note that these models are not necessarily representative of PSNs. Instead, they are general-purpose models. This is intentional, because the models that we use are intended to illustrate wide applicability of our approach to any domain where data can be modeled as networks. It is our subsequent analyses on real-world PSNs that will focus specifically on the task of PC.

First, we evaluate the considered approaches on synthetic networks of the same size but of different labels (originating from the three network models). To evaluate the robustness of our PC framework to the choice of network size, we repeat this analysis three times, by increasing the size of the considered networks. That is, we perform three separate analyses of three different network data sets, where in a given data set, all networks are of the same size, and one third of the networks in the set comes from each of the three network models. We denote these network sets as *Synthetic-100*, *Synthetic-500*, and *Synthetic-1000* (Table 1), where each set consists of 50 networks per model (totaling to  $50 \times 3 = 150$  networks). The numbers of nodes and edges in these networks are chosen in a way so that the networks closely mimic sizes of real-world PSNs.

Second, we evaluate the considered approaches on networks of different sizes as well as different labels, to check whether the approaches can correctly identify as similar networks from the same model despite the networks being of different sizes, as well as that they can correctly identify as dissimilar networks from different models despite the networks being of the same size. To generate a synthetic network set of different sizes, we combine networks from *Synthetic-100*, *Synthetic-500*, and *Synthetic-1000* together. We denote the combined network set as *Synthetic-all* (Table 1).

**Real-world PSNs with CATH categorization.** Each protein in ProteinPDB (defined above) is composed of 3D coordinates of the heavy atoms of its amino acids. Given a protein, we use the 3D coordinate information to compute Euclidean distance between each pair of amino acids, i.e., between any of their heavy atoms. Then, we construct a PSN in which nodes represent amino acids and edges connect pairs of amino acids that are sufficiently close (i.e. within a given distance cut-off) in the protein's 3D structure. Again, we emphasize that two amino acids are sufficiently close if any of the heavy atoms of the first amino acid and any of the heavy atoms of the second amino acid are within a given distance cut-off. While effective definitions of contact between amino acids may differ from fold to fold<sup>35</sup>, we use the suggested distance cut-off of 4 Å<sup>15</sup>. ProteinPDB contains 17,884 protein domains that have CATH categorization, which results in 17,884 PSNs. Of these PSNs, to ensure that PSNs are of reasonable "confidence", we focus for further analyses on those PSNs that meet all of the following criteria: 1) the given network has more than 100 nodes, 2) the maximum diameter of the network is more than five, and 3) the network is composed of a single connected component. This results in 9,509 such PSNs.

First, we test how well the considered approaches can compare PSNs belonging to the top hierarchical categories of CATH (i.e.,  $\alpha$ ,  $\beta$ , and  $\alpha/\beta$ ). Of the 9,509 PSNs, 2,628, 3,085, and 3,796 PSNs belong to (i.e., are labeled with)  $\alpha$ ,  $\beta$ , and  $\alpha/\beta$  categories, respectively. We denote this set as *CATH-primary*. The set contains a large enough number of PSNs in each category, which ensures enough statistical power for further analyses.

Second, we test how well the approaches can compare PSNs belonging to the secondary hierarchical categories of CATH. To ensure enough statistical power for further analyses, we pick all secondary categories of  $\alpha$ ,  $\beta$ , and  $\alpha/\beta$  that comprise of at least 30 PSNs. We denote these three sets as *CATH- $\alpha$* , *CATH- $\beta$* , and *CATH- $\alpha/\beta$* , respectively. *CATH- $\alpha$*  consists of four secondary  $\alpha$  categories (i.e., labels), with an average of 656 PSNs per category. *CATH- $\beta$*  consists of 10 secondary  $\beta$  categories, with an average of 297 PSNs per category. *CATH- $\alpha/\beta$*  consists of 4 secondary  $\alpha/\beta$  categories, with an average of 948 PSNs per category. For details, see Table 1 and Supplementary Table S2.

**Real-world PSNs with SCOP categorization.** ProteinPDB has 15,762 protein domains with SCOP categorization, which results in 15,762 PSNs. Of these PSNs, to ensure that PSNs are of reasonable "confidence", we focus for further analyses on 11,451 PSNs that meet all of the above criteria while forming PSNs with CATH categorization.

Per our above strategy (when analyzing PSNs with CATH categorization), first, we evaluate how well the considered approaches can compare PSNs from the top hierarchical categories of SCOP (i.e.  $\alpha$ ,  $\beta$ ,  $\alpha/\beta$ ,  $\alpha+\beta$ , coiled coil, membrane, and multi-domain). Of the 11,451 PSNs, 1,678, 2,541, 3,835, 2,879, 44, 156, and 318 PSNs belong to  $\alpha$ ,  $\beta$ ,  $\alpha/\beta$ ,  $\alpha+\beta$ , coiled coil, membrane, and multi-domain categories, respectively. This set, denoted as *SCOP-primary*, contains enough PSNs in each category to ensure enough statistical power for further analyses.

Second, we evaluate how well the approaches can compare PSNs belonging to the secondary hierarchical categories of SCOP. To ensure enough statistical power, we pick all secondary categories of  $\alpha$ ,  $\beta$ ,  $\alpha/\beta$ ,  $\alpha+\beta$ , coiled coil, membrane, and

Data set			Number of		
Type	Size	Name	Networks	Nodes	Edges
Synthetic networks	Same	Synthetic-100	150	100	400
		Synthetic-500	150	500	2,000
		Synthetic-1000	150	1,000	4,000
	Different	Synthetic-all	450	100-1,000	400-4,000
Real-world PSNs	Same	CATH-95	24	95	343-362
		CATH-99	28	99	347-374
		CATH-251-265	16	251-265	1,003-1,076
	Different	CATH-primary	9,509	101-872	243-3,849
		CATH- $\alpha$	2,628	101-872	320-3,849
		CATH- $\beta$	3,085	101-559	243-2,166
		CATH- $\alpha/\beta$	3,796	101-759	288-3,507
		SCOP-primary	11,451	101-1,381	105-5,558
		SCOP- $\alpha$	1,678	101-938	147-4,082
		SCOP- $\beta$	2,541	101-581	111-2,113
		SCOP- $\alpha/\beta$	3,835	101-904	105-3,966
		SCOP- $\alpha+\beta$	2,879	101-696	120-3,064
		SCOP-multidomain	318	196-1,256	767-5,558

**Table 1.** Synthetic network and real-world PSN data sets that we use. For the given data set, the second column indicates whether its networks are of the same size or different sizes, and the last three columns indicate the number of its networks as well as their size(s) in terms of the number of nodes and edges. For more details, see Supplementary Table S2.

multi-domain that comprise of at least 30 PSNs. We denote these five sets as  $SCOP-\alpha$ ,  $SCOP-\beta$ ,  $SCOP-\alpha/\beta$ ,  $SCOP-\alpha+\beta$ , and  $SCOP-multidomain$ , respectively.  $SCOP-\alpha$  consists of 16 secondary  $\alpha$  categories, with an average of 57 PSNs per category.  $SCOP-\beta$  consists of 21 secondary  $\beta$  categories, with an average of 88 PSNs per category.  $SCOP-\alpha/\beta$  consists of 26 secondary  $\alpha/\beta$  categories, with an average of 113 PSNs per category.  $SCOP-\alpha+\beta$  consists of 28 secondary  $\alpha+\beta$  categories, with an average of 57 PSNs per category.  $SCOP-multidomain$  consists of 2 secondary multi-domain categories, with an average of 63 PSNs per category. For details, see Table 1 and Supplementary Table S2.

**Real-world PSNs of the same size.** To ensure that PC is not biased by PSN size, we need a data set with PSNs of the same (or similar) network size. Hence, focusing on PSNs of  $\alpha$  and  $\beta$  categories from the CATH-primary data set, we infer three such same-size PSN data sets, denoted as  $CATH-95$ ,  $CATH-99$ , and  $CATH-251-265$  (Table 1 and Supplementary Section S1.1).

## 2.3 Our graphlet PCA framework

### 2.3.1 The PCA framework

The novelty of our new PCA framework comes from using graphlet-based measures in the task of PC (Fig. 1). Yet, the framework is generalizable, as it can use any measure(s). Namely, given a network data set and a measure of network topology (see below), we compute one vector per network per measure. We perform PCA (a standard dimension reduction technique) on the resulting vectors to compute principal components for each network. We pick the first  $r$  principal components, where the value of  $r$  is at least two and as low as possible so that the  $r$  components account for at least 90% of variation in the data. For every pair of networks  $N_i$  and  $N_j$ , we compute their cosine similarity,  $s^{cos}(N_i, N_j)$ , based on the networks' first  $r$  principal components. We convert the similarity into distance as  $d^{cos}(N_i, N_j) = 1 - s^{cos}(N_i, N_j)$ . We use the PCA-based distances to hypothesize that same-label networks will be close in the PCA space while networks of different labels will be distant. Like most of the network approaches from Fig. 1, our approach performs *alignment-free* network comparison, i.e., it does *not* need to align nodes between the compared networks before it can quantify their similarity, as *alignment-based* approaches do<sup>36</sup>.

### 2.3.2 Our graphlet measures

Graphlets are small connected *induced* subgraphs (Fig. 2). They have been proven as sensitive and superior measures of topology in numerous contexts when studying protein-protein interaction networks<sup>16,24-26,37,38</sup>. Hence, we use graphlets as PSN measures for PC, as follows.

**Graphlet counts.** We count occurrences of each graphlet on up to  $n$  nodes in the given network. To investigate the best choice for  $n$ , we use counts for 3-4-node (Fig. 2) and 3-5-node graphlets, resulting in *Graphlet-3-4* and *Graphlet-3-5* measures, respectively. Graphlet counts typically vary by orders of magnitude in real-world networks<sup>25</sup>. Hence, we normalize graphlet counts by taking their logarithms. Here, we do not consider 3-node-only graphlets, because there are only two 3-node graphlets, which may not be suitable for our PCA framework, and also because using up to 4- or 5-node graphlets improves accuracy upon using only 3-node graphlets<sup>27-29</sup>.

**Normalization of graphlet counts.** Networks with similar topology can have dissimilar graphlet counts simply because of their dissimilar network sizes (see Results). To remove the bias of PSN size, we normalize graphlet counts by scaling them between 0 and 1. Formally, given a network, let  $g_1, g_2, \dots, g_n$  be counts of  $n$  graphlets  $G_1, G_2, \dots, G_n$ , respectively ( $n = 8$  for



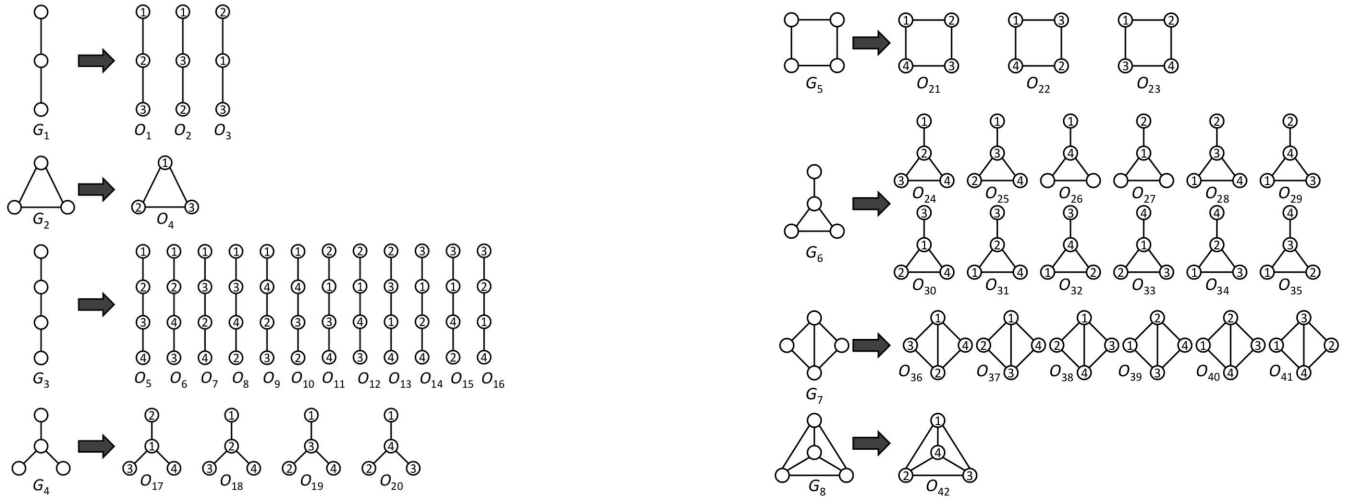


**Figure 2.** All possible eight regular (non-ordered) 3-4-node graphlets ( $G_1, G_2, \dots, G_8$ ; on the left of the given arrow) and their corresponding 42 ordered graphlets ( $O_1, O_2, \dots, O_{42}$ ; on the right of the given arrow).

3-4-node graphlets and  $n = 29$  for 3-5-node graphlets). We normalize count  $g_i$  of graphlet  $G_i$  as  $g_i / \sum_{j=1}^n g_j$ . We denote the normalized Graphlet-3-4 and Graphlet-3-5 measures as *NormGraphlet-3-4* and *NormGraphlet-3-5*, respectively.

**Integration of graphlets with protein sequences: ordered graphlet counts.** While amino acids appear in a particular order in the sequence, graphlets were originally not designed to capture this node order information. For example, nodes in graphlet  $G_1$  can appear in three different orders (Fig. 2), but  $G_1$  cannot differentiate between them. To take advantage of both network and sequence data, *ordered graphlets* were recently proposed<sup>16</sup>, which embed the *relative* order of nodes onto graphlets. For example, the three different orders of graphlet  $G_1$  were formulated as three different ordered graphlets:  $O_1, O_2$ , and  $O_3$  (Fig. 2). This way, Malod-Dognin and Pržulj<sup>16</sup> defined all four possible 3-node ordered graphlets for all two possible 3-node “regular” (i.e., original non-ordered) graphlets.

We denote the measure consisting of the existing four counts for 3-node ordered graphlets as *OrderedGraphlet-3*, and we denote our normalized counterpart of *OrderedGraphlet-3* as *NormOrderedGraphlet-3* (normalization is done in the same way as explained above). Unlike for regular (non-ordered) graphlets, we *do* consider 3-node-only ordered graphlets within our PCA approach. We do this to fairly compare our alignment-free PCA approach with the existing alignment-based non-PCA approach by Malod-Dognin and Pržulj<sup>16</sup> that can support only 3-node ordered graphlets. To benefit from larger graphlets, we *extend* this idea to include within our PCA approach all 38 possible 4-node ordered graphlets for all six possible 4-node regular graphlets on top of the existing four 3-node ordered graphlets. We denote the resulting measure consisting of 42 ordered graphlet counts for 3-4-node graphlets (Fig. 2) as *OrderedGraphlet-3-4* and its normalized counterpart as *NormOrderedGraphlet-3-4*. Inclusion of ordered graphlets on five nodes would cause the number of graphlets to grow significantly (e.g., graphlet  $G_9$  can be formulated as 60 different ordered graphlets). Since using too many measures often causes overfitting, which can eventually lead to increased error rate<sup>39</sup>, we do not consider 5-node ordered graphlets. Note that ordered graphlet counts do not vary by orders of magnitude in our data as regular graphlet counts do, so we do not take their logarithms.

While ordered graphlets capture relative sequence positions of interacting amino acids, they do not capture how far those amino acids are in the sequence. While there have been conflicting findings regarding the effect of long-range interactions on secondary structure prediction accuracy<sup>6</sup>, we hypothesize that amino acids that are close enough in the protein 3D structure but are far away in the protein sequence are more important than amino acids that are close enough in the 3D structure simply because they are also close in the sequence. To capture and evaluate this hypothesis, we propose a novel concept of “*long-range(K)*” *ordered graphlets*, where the “long-range( $K$ )” constraint is introduced so that a given ordered graphlet is identified in the given PSN if and only if: 1) the same ordered graphlet would also be identified in the above described analysis, and 2) every pair of amino acids that are linked by an edge in the graphlet are at least  $K$  distance apart in the sequence (that is,  $K$  is the absolute difference between sequence positions of two amino acids of interest). See Fig. 3 for an illustration of this concept. Clearly, all graphlets identified under the “long-range( $K$ )” ordered graphlet approach will also be identified under the traditional ordered graphlet approach, but the opposite is not necessarily true. As a proof of concept, we apply the concept of “long-range( $K$ )” ordered graphlets on the *NormOrderedGraphlet-3-4* (which as we will show in Results is the best of all graphlet features) and we denote the new measure as *NormOrderedGraphlet-3-4(K)*. To evaluate the performance of

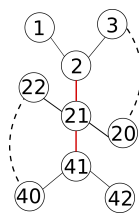


**Figure 3.** Illustration of the importance of “long-range( $K$ )” ordered graphlets. A PSN is shown for a toy protein that consists of 42 amino acids in the sequence, i.e., nodes in the PSN (amino acids 4–19 and 23–39 are not shown for simplicity, as indicated by dashed lines). The nodes are denoted by their amino acid positions in the sequence. Black solid lines are network edges that indicate sequence closeness of the corresponding amino acids (meaning that the amino acids are adjacent in the sequence), which in turn yields sufficient 3D spatial proximity of the amino acids. On the other hand, red solid lines are network edges that indicate only spatial proximity, without sequence adjacentness. On the one hand, both the three-node path 1–2–3 as well as the three-node path 2–21–41 correspond to the same ordered graphlet, namely  $O_1$  from Fig. 2, under the traditional ordered graphlet approach. However, we argue that the latter is more interesting than the former, as the former is  $O_1$  simply because of sequence adjacentness of amino acids 1 and 2 as well as 2 and 3, while the latter is  $O_1$  because of spatial proximity of amino acids 2 and 21 as well as 21 and 41. On the other hand, even for  $K$  value as low as two, the path 1–2–3 will not be detected as  $O_1$  under the “long-range( $K$ )” ordered graphlet approach, while the path 2–21–41 will, because all of its linked node pairs are at least two amino acids apart in the sequence. Note that the path 2–21–41 will be identified as  $O_1$  up to  $K$  value of  $\min(21 - 2, 41 - 21) = 19$ .

*NormOrderedGraphlet-3-4( $K$ )*, we vary  $K$  from one to 10 in increments of one and from 10 to 35 in increments of five. Then, for each considered data set, we report results for the value of  $K$  that results in the best PC accuracy (for details, see Results).

## 2.4 Existing approaches

We use 15 existing *network*, *3D contact*, and *sequence* approaches in the task of PC (Fig. 1).

### 2.4.1 Existing network approaches

Existing approaches of this type that we use for PC (not all of which were proposed for PC but can be adapted to it) can be categorized into graphlet and non-graphlet approaches. None of them use PCA as we do.

**Existing graphlet approaches.** These include graphlet degree distribution agreement (GDDA)<sup>26</sup>, relative graphlet frequency distance (RGFD)<sup>25</sup>, graphlet correlation distance (GCD)<sup>40</sup>, and GR-align<sup>16</sup>. Among them, GDDA, RGFD, and GCD can compare any type of networks, while GR-align has been specifically designed to compare PSNs. GDDA, RGFD, and GCD are alignment-free network comparison approaches, while GR-align is an alignment-based approach. In particular, it was the GR-align study<sup>16</sup> that introduced the idea of 3-node-only ordered graphlets, which we partly base our approach on.

Two alternative graphlet approaches were used in the context of PSNs<sup>41,42</sup>, but they were used to predict (classify in a supervised manner) functional residues in PSNs (where residues are nodes in PSNs) and not for PSN comparison. Since these approaches compare nodes rather than networks, and since they are supervised (while our study is unsupervised, per our discussion below), the approaches do not fit the context of our study. As such, we do not consider them further.

**Existing non-graphlet approaches.** Several PSN measures have already been used for PC: *average degree*, *average distance*, *maximum distance*, *average closeness centrality*, *average clustering coefficient*, *intra-hub connectivity*, and *assortativity* (Supplementary Section S1.2)<sup>8,17–20</sup>. For each measure, for each pair of networks, we compute Euclidean distance between the networks’ vectors (because all vectors are 1-dimensional, here we cannot use cosine similarity as for our approach).

We combine the seven measures into an eighth measure, *Existing-all*, to investigate whether the integration of different and complementary topological measures helps PC. We use Existing-all within our PCA framework. This way, we can fairly compare our graphlet measures and the existing non-graphlet measures within the same framework.

### 2.4.2 Existing 3D contact approaches

These include DaliLite<sup>13</sup> and TM-align<sup>14</sup>, both of which are alignment-based.

### 2.4.3 Existing sequence approaches

Mizianty et al.<sup>4</sup> used protein length and amino acid propensities to define a sequence measure, which outperformed methodologies of 11 other methodologies<sup>4</sup>. Thus, we use this measure, denoted as *Sequence*, within our PCA framework. This way, we can fairly compare network and sequence measures within the same framework.

## 2.5 Evaluation of PC accuracy

Given a set of objects (proteins or networks) with known labels, for a good approach, the distance between objects of the same label should be small, while the distance between objects of different labels should be large. To evaluate this, we rely on an established unsupervised strategy<sup>36</sup>. By “unsupervised”, we mean that we rely on object labels only in the phase of evaluating a method’s output. That is, we do not use any label information to train the given method or produce its output, as a supervised (classification) approach would do. Details of our evaluation are as follows. For each approach, we first compute the distance between each pair of objects according to the given PC approach. Then, we sort all object pairs in terms of their increasing distance and consider  $k$  closest object pairs, where we vary  $k$  from 0% to 100% in increments of 0.1%. Next, we compute the accuracy in terms of *precision* and *recall*, where precision is the fraction of label-matching object pairs out of the considered object pairs, and recall is the fraction of the considered label-matching object pairs out of all label-matching object pairs. To summarize the precision and recall results over the whole [0-100%] range of  $k$ , we measure overall accuracy of the given PC approach by computing AUPR. Alternatively, we compute the accuracy in terms of *sensitivity* and *specificity*, where sensitivity is the fraction of the considered label-matching object pairs out of all label-matching object pairs, and specificity is the fraction of the considered non-label-matching object pairs out of all non-label-matching object pairs. To summarize the sensitivity and specificity results over the whole [0-100%] range of  $k$ , we measure overall accuracy of the given approach by computing AUROC. Given a data set, we compare different approaches by comparing their AUPR or AUROC scores.

## 3 Results

### 3.1 Comparison of synthetic networks

The motivation behind evaluating our approach against the existing ones on synthetic networks is to demonstrate the general applicability of our approach to any domain where data can be modeled with networks. This is important, because some of the existing approaches that we evaluate against have already been used in tasks different than our considered task of PC. So, if we can demonstrate the superiority of our approach over such widely applicable existing approaches, then this would imply that henceforth it is our approach that should be used in those tasks instead.

Unlike for real-world PSNs, for synthetic networks, we cannot evaluate 3D contact and sequence approaches, as they require 3D contact and sequence information, respectively, which synthetic networks do not contain. Thus, we can only apply network approaches to synthetic networks, with the exception of ordered graphlet approaches, including GR-align, that require some node order, which again synthetic networks do not have. We evaluate the remaining (15) network approaches on synthetic networks. For these networks, the topology-based ground truth label categorization is known. (Note that a random network model that would, unlike the existing general-purpose random network models that we use, generate synthetic networks with embedded node order which would closely mimic all of protein sequence, 3D, and network structure, would fit better the context of PSN comparison than the general-purpose models that we use. However, developing such a model is non-trivial and is thus out of the scope of the current study.)

First, we evaluate the network approaches (i.e., their existing versions that are non-normalized in terms of network size) on synthetic networks of the same size. Second, we evaluate whether the current non-normalized versions of the network approaches can successfully cope with synthetic networks of different sizes. We find that our graphlet PCA approach overall outperforms the existing network approaches, including the existing graphlet (non-PCA) approaches. Therefore, in all subsequent tests, we focus on the graphlet PCA methodology. Yet, the accuracy of the graphlet PCA approach (as well as every other approach) drops when analyzing networks of different sizes compared to analyzing networks of the same size, meaning that some level of miscategorization arises due to the networks having different sizes. This indicates a need for devising a normalized version of the graphlet PCA approach. Thus, third, we develop such a normalized approach, and as we show, normalization indeed improves PC. Forth, we summarize our key findings resulting from analyzing the synthetic network data. The four items are discussed in the following four subsections.

#### 3.1.1 Evaluation of non-normalized network measures

Here, we evaluate non-normalized versions of our graphlet PCA approach (i.e., Graphlet-3-4 and Graphlet-3-5), existing graphlet approaches (i.e., GDDA, RGFD, and GCD), and existing non-graphlet approaches (i.e., average degree, average distance, maximum distance, average closeness centrality, average clustering coefficient, intra-hub connectivity, assortativity, and Existing-all). We evaluate the approaches on synthetic network data of the same size (i.e., Synthetic-100, Synthetic-500, and Synthetic-1000). For details, see Methods.

For each data set, both non-normalized versions of our graphlet PCA approach outperform the existing graphlet and non-graphlet approaches, as the former two achieve 100% accuracy (Table 2 and Supplementary Table S2). Some of the existing



Approach	Synthetic			
	Synthetic-100	Synthetic-500	Synthetic-1000	Synthetic-All
Graphlet-3-4	<b>100.00</b>	<b>100.00</b>	<b>100.00</b>	81.76
Graphlet-3-5	<b>100.00</b>	<b>100.00</b>	<b>100.00</b>	83.28
NormGraphlet-3-4	<b>100.00</b>	<b>100.00</b>	<b>100.00</b>	94.37
NormGraphlet-3-5	<b>100.00</b>	<b>100.00</b>	<b>100.00</b>	<b>99.86</b>
GDDA	97.36	<b>100.00</b>	99.99	91.46
RGFD	<b>100.00</b>	<b>100.00</b>	<b>100.00</b>	98.55
GCD	89.26	<b>100.00</b>	<b>100.00</b>	86.27
Average degree	79.76	79.76	79.76	68.77
Average distance	82.47	98.12	99.60	57.10
Maximum distance	68.82	84.32	93.08	46.11
Average closeness centrality	86.10	88.46	85.33	48.41
Average clustering coefficient	98.93	99.68	99.25	79.37
Intra-hub connectivity	70.88	69.11	69.31	66.61
Assortativity	82.79	92.27	91.73	81.98
Existing-all	<b>100.00</b>	<b>100.00</b>	<b>100.00</b>	85.92

**Table 2.** Accuracy with respect to AUPRs (expressed as percentages) on synthetic networks. Results for non-normalized approaches are highlighted in 1) light gray for network data of the same size and 2) dark gray for network data of different sizes. Results for normalized approaches are not highlighted. Given a network data set (within a column), the AUPR of the best approach is shown in bold. For equivalent results with respect to AUROCs, see Supplementary Table S2.

methods also achieve 100% accuracy on some of the data sets, but only one (RGFD) does so on all three data sets and is thus comparable to our approach. However, as we show below, RGFD loses its comparable performance in other tests.

Both our graphlet PCA approach and the existing graphlet (non-PCA) approaches outperform the existing non-graphlet approaches (Table 2 and Supplementary Table S2). This confirms the power of the local graphlets over the global network measures that have traditionally been used for PC.

Combining the seven existing non-graphlet measures into Existing-all and using Existing-all in our PCA framework improves the accuracy of each individual non-graphlet measure. This confirms that measure integration helps, which is why we have developed our framework to allow for this in the first place. Existing-all is comparable to our graphlet PCA approach (Table 2 and Supplementary Table S2). However, Existing-all loses its comparable performance in other tests (see below).

### 3.1.2 Network size affects comparison via non-normalized measures

To test whether the non-normalized versions of our graphlet PCA approach, existing graphlet approaches, and existing non-graphlet approaches, all of which are non-normalized, are robust to the size of networks to be compared, we evaluate the approaches on the Synthetic-all set, which contains networks with different topologies *and* of different sizes (unlike the equal-size network sets from the above analysis). In this analysis, we observe a decline in accuracy for each approach (Table 2 and Supplementary Table S2). Clearly, the accuracy is biased by network size.

### 3.1.3 Normalization of graphlet measures improves comparison

Motivated by this network size-related bias of all non-normalized network measures, we propose a normalized version of the best of all measures, namely our graphlet PCA measures. We validate our normalized graphlet PCA measures as follows. When we apply them to Synthetic-100, Synthetic-500, and Synthetic-1000, we hope to preserve the maximum (100%) accuracy for the three network data sets of the same size while improving the accuracy for Synthetic-all that contains networks of different sizes. Indeed, this is exactly what we observe (Table 2 and Supplementary Table S2). Now the best of our graphlet PCA approaches (i.e., NormGraphlet-3-5) outperforms each of the three existing graphlet (non-PCA) approaches, even though all of these approaches are based on graphlets. This shows the usefulness of our PCA framework as a whole over the existing graphlet methodologies. Also, now NormGraphlet-3-5 outperforms the non-graphlet Existing-all approach under the same PCA framework, which confirms the power of graphlets.

### 3.1.4 Summary of results for synthetic networks

Our (non-normalized) graphlet PCA measures overall outperform the existing graphlet (non-PCA) approaches, which in turn outperform the existing non-graphlet approaches. Our normalized graphlet PCA measures further improve upon their non-normalized counterparts (and thus upon the existing approaches). NormGraphlet-3-5 is the most accurate approach.

## 3.2 Comparison of PSNs

In our analysis of real-world PSNs, for which CATH- or SCOP-label-based (rather than topology-based as above) ground truth label categorization is known, first, we evaluate the approaches (i.e., their existing versions that are non-normalized in terms of network size) on PSNs of the same size. Second, we test the approaches on PSNs of different sizes. In both tests, overall,

our graphlet PCA approach is superior to the existing approaches. Yet, the accuracy of all approaches drops when analyzing PSNs of different sizes compared to analyzing PSNs of the same size. Therefore, third, we test whether graphlet normalization improves PC. Indeed, this is what we observe. Fourth, to investigate whether the integration of network topology with protein sequences can improve PC, we test our ordered graphlet PCA approach, including the effect of the “long-range( $K$ )” constraint. Fifth, we compare the considered approaches in terms of their running times. Sixth, we summarize our key findings resulting from analyzing the PSN data. The six items are discussed in the following six subsections.

### 3.2.1 Evaluation of non-normalized measures

Here, we benchmark the non-normalized versions of our PCA graphlet approach, existing graphlet (non-PCA) approaches, existing non-graphlet approaches, and 3D contact approaches on all PSN data sets for which networks within the given set are of the same size, i.e., on CATH-95, CATH-99, and CATH-251-265. For each PSN set, just as for the synthetic networks, the non-normalized versions of our graphlet PCA approach (Graphlet-3-4 and Graphlet-3-5) are superior to the existing graphlet, non-graphlet, and 3D contact approaches, except one (RGFD) that is comparable to our approach (Table 3 and Supplementary Table S3). Yet, as we show below, RGFD loses its comparable performance in other tests. Again, combining the seven existing non-graphlet measures into Existing-all typically improves the accuracy of each individual measure (Table 3). Existing-all is comparable to the two non-normalized versions of our graphlet PCA approach. However, as we show below, Existing-all loses its comparable performance in other tests.

### 3.2.2 Network size affects comparison via non-normalized measures

Next, we evaluate the same non-normalized approaches on all 10 sets of PSNs of different sizes (i.e., CATH-primary, CATH- $\alpha$ , CATH- $\beta$ , CATH- $\alpha/\beta$ , SCOP-primary, SCOP- $\alpha$ , SCOP- $\beta$ , SCOP- $\alpha/\beta$ , SCOP- $\alpha+\beta$ , and SCOP-multidomain). We observe a decline in accuracy for each approach, which confirms the bias of network size. Nonetheless, the non-normalized versions of our graphlet PCA approach remain superior or comparable to all existing methods (Table 3 and Supplementary Table S3).

### 3.2.3 Normalization of graphlet measures improves comparison

Motivated by the above network size-related bias of all considered non-normalized approaches, we propose a normalized version of the best of those approaches, namely of the graphlet PCA measures. When we apply each of the normalized measures to the PSN data, we hope to ideally improve or at least preserve the accuracy on the PSN data sets of the same network size (i.e., CATH-95, CATH-99, and CATH-251-265) while improving the accuracy for the 10 sets of PSNs of different sizes, compared to the accuracy of the measures’ non-normalized counterparts. Indeed, this is exactly what we observe (Table 3 and Supplementary Table S3).

### 3.2.4 Integration of network and sequence data via ordered graphlets

The versions of our PCA approach that are based on regular (non-ordered, as considered thus far) graphlets, already perform much better than the sequence approach (Table 3 and Supplementary Table S3). Integration of network data with sequence data may further improve the accuracy compared to only network and only sequence approaches. We test this by using ordered graphlets to impose the sequence-based order of amino acids onto nodes in regular graphlets (Fig. 2).

Considering only non-normalized graphlet measures, ordered graphlets (i.e., OrderedGraphlet-3 and OrderedGraphlet-3-4) improve upon their regular graphlet counterparts for PSNs of the same size as well as of different sizes (Table 3). Considering also normalized graphlet measures, NormOrderedGraphlet-3-4 leads to better accuracy compared to its non-normalized counterpart, though NormOrderedGraphlet-3 does not improve upon its non-normalized counterpart (Table 3).

Integrating the “long-range( $K$ )” constraint on top of *NormOrderedGraphlet-3-4*, i.e., considering *NormOrderedGraphlet-3-4( $K$ )*, further improves accuracy (Table 3 and Supplementary Table S3). Recall that in these tests, we vary  $K$  (see Methods). The best value of  $K$  is data set-dependent. Of the 13 considered data sets, increasing  $K$  to at least two (i.e., considering the “long-range( $K$ )” ordered graphlet approach) helps compared to  $K = 1$  (i.e., compared to the traditional ordered graphlet approach) for the majority (seven) of the data sets (Supplementary Tables S4 and S5). In particular, there is significant increase in accuracy for all data sets corresponding to the secondary hierarchical categories of CATH (except CATH- $\beta$ ) and SCOP. For the seven data sets, the best value of  $K$  ranges from three to 35. Since even as high value of  $K$  as 35 yields better accuracy than smaller values of  $K$ , these results exemplify the importance of long-range interactions in the task of PC.

The fact that within our PCA framework ordered graphlets beat regular graphlets alone and the sequence approach alone confirms that PSN data and sequence data are complementary and should thus be integrated. We consider this to be one of our key contributions. Here, we note that 3-node-only ordered graphlets *were* used for protein 3D structural alignment within

**Table 3.** Accuracy with respect to AUPRs (expressed as percentages) on real-world PSN data sets of the same network size as well as of different network sizes. Results for non-normalized approaches are highlighted in 1) light gray for network data of the same size and 2) dark gray for network data of different sizes. Results for normalized approaches are not highlighted. Given a network data set (within a given column), the AUPR of the best approach is shown in bold. For equivalent results with respect to AUROCs, see Supplementary Table S3.

Approach	CATH of the same size			CATH (of different sizes)				SCOP (of different sizes)					
	CATH-95	CATH-99	CATH-251-265	primary	$\alpha$	$\beta$	$\alpha/\beta$	primary	$\alpha$	$\beta$	$\alpha/\beta$	$\alpha+\beta$	Multi domain
Graphlet-3-4	82.28	92.05	92.35	47.47	50.53	38.50	46.62	37.85	19.95	32.59	21.68	15.37	63.46
Graphlet-3-5	83.31	92.78	92.89	47.86	50.46	37.78	45.77	37.29	19.57	26.47	17.99	12.77	63.86
OrderedGraphlet-3	90.99	95.93	91.02	45.75	52.19	42.04	<b>49.69</b>	35.33	21.71	44.71	19.80	20.24	60.37
OrderedGraphlet-3-4	96.69	91.88	97.20	46.16	52.39	40.50	48.38	33.60	20.72	39.78	17.37	16.29	60.19
NormGraphlet-3-4	96.03	<b>100.00</b>	95.28	52.57	50.93	37.59	43.24	36.89	17.15	23.75	18.59	13.66	68.95
NormGraphlet-3-5	94.11	99.73	97.67	53.24	51.02	37.21	43.74	37.51	17.31	23.55	18.03	9.85	67.51
NormOrderedGraphlet-3	83.54	96.49	93.51	54.2	52.79	47.24	33.5	33.36	15.26	18.72	12.95	9.39	67.23
NormOrderedGraphlet-3-4	<b>97.59</b>	96.58	<b>98.74</b>	<b>65.64</b>	53.05	49.11	44.34	<b>44.50</b>	21.75	26.23	16.68	19.92	72.70
NormOrderedGraphlet-3-4(K)	<b>97.59</b>	96.58	<b>98.74</b>	<b>65.64</b>	<b>53.41</b>	49.11	48.31	<b>44.50</b>	<b>31.63</b>	38.83	<b>34.35</b>	33.84	<b>82.02</b>
GDDA	77.65	80.78	71.46	42.77	49.09	34.36	34.15	32.09	14.77	9.99	11.92	5.77	66.79
RGFD	87.87	89.49	94.00	53.75	51.26	42.15	41.77	38.86	17.42	21.15	12.90	9.76	66.21
GCD	71.70	74.92	77.23	42.61	49.99	37.00	31.26	31.78	14.20	11.46	10.62	6.37	68.33
GR-align	76.25	65.03	70.25	39.07	52.68	<b>50.11</b>	45.03	28.55	30.05	<b>59.07</b>	24.17	<b>41.17</b>	77.43
Average degree	48.22	50.21	61.22	42.81	50.22	37.16	38.55	30.85	11.54	14.31	11.12	5.98	60.37
Average distance	64.49	60.22	51.60	35.13	50.99	38.61	34.78	29.75	12.51	24.76	14.06	8.21	72.98
Maximum distance	62.39	73.49	54.89	35.07	49.59	37.35	39.78	29.67	15.50	19.21	13.95	8.37	58.33
Average closeness centrality	62.73	60.94	45.73	34.67	49.86	36.60	39.55	27.84	12.23	21.32	11.58	7.55	70.54
Average clustering coefficient	87.01	72.10	89.96	44.15	49.19	39.17	32.28	30.77	11.47	16.26	10.58	6.61	63.47
Intra-hub connectivity	54.94	72.34	63.76	34.79	50.14	36.85	40.04	29.21	11.87	23.41	14.26	10.66	64.51
Assortativity	76.97	85.34	93.31	37.41	48.10	35.90	30.64	26.99	8.98	12.11	9.02	5.18	54.93
Existing-all	82.14	91.56	92.48	47.69	50.46	36.53	41.35	35.68	19.49	23.56	14.16	9.33	76.35
DaliLite	53.38	69.12	58.96	39.84	49.22	46.34	39.33	31.64	18.63	27.85	22.16	13.04	70.22
TM-align	50.93	62.02	45.79	37.30	45.56	34.77	28.63	25.78	8.05	16.99	11.45	7.55	58.18
Sequence	70.23	62.14	54.48	40.45	50.24	37.66	35.18	29.02	22.13	20.74	11.82	11.77	73.78

the GR-align approach. We adopt the existing idea of 3-node ordered graphlets but we do so within our alignment-free PCA framework as opposed to the existing alignment-based GR-align approach. Also, we extend this idea into larger, 3-4-node ordered graphlets. Further, we add a “long-range( $K$ )” constraint into the process of ordered graphlet counting. Importantly, when we consider 3-node-only ordered graphlets within our PCA framework, which makes the comparison with GR-align as fair as possible, our PCA approach is superior to GR-align (Table 3). This is further supported when we compare the accuracy rankings of the different methods over all PSN sets (Table 4). When we also consider larger ordered graphlets, this further improves the performance of our PCA approach, and so does the “long-range( $K$ )” ordered graphlet constraint (Tables 3 and 4). GR-align is also slower than our approach. For example, it is 25 times slower than the fairly comparable 3-node-only ordered graphlet version of our PCA approach (Table 4). These results validate our PCA framework as a whole. Note that when one’s goal is not just to quantify the level of similarity between networks but also to map nodes between the networks, using an alignment-free approach such as our graphlet PCA framework is inappropriate, and instead, an alignment-based approach such as GR-align needs to be used. For details on alignment-free versus alignment-based approaches, see Yaveroglu *et al.*<sup>36</sup>.

Another of our key contributions is that even our regular graphlet PCA approaches and especially their normalized and (“long-range( $K$ )”) ordered counterparts are superior to traditional 3D contact approaches, even though both approach types (network vs. 3D contact) use 3D structural information. This highlights the usefulness of network analyses of protein structures. This is especially true given that our network approaches are also faster than the 3D contact approaches, as follows.

### 3.2.5 Running time comparison

All alignment-free network approaches are comparable in terms of running time to each other as well as to the sequence approach, they are followed by the only alignment-based network approach (GR-align), and all of them are significantly faster than the 3D contact approaches (Table 4).

### 3.2.6 Summary of results for PSNs

The non-normalized versions of our graphlet PCA approach are superior to the existing graphlet (non-PCA), non-graphlet, 3D contact, and sequence approaches. By normalizing the graphlet measures, we improve upon the non-normalized measures and

Approach	AUPR		AUROC		Running time (hrs)
	Rank	<i>p</i> -value	Rank	<i>p</i> -value	
Graphlet-3-4	8.38	9.42e-05	10.50	0.000147	0.43
Graphlet-3-5	9.00	4.81e-06	10.40	8.74e-05	0.49
OrderedGraphlet-3	7.15	0.00225	9.92	0.000692	0.38
OrderedGraphlet-3-4	7.31	0.00143	8.69	0.0018	2.39
NormGraphlet-3-4	7.77	3.57e-05	8.15	0.000156	0.44
NormGraphlet-3-5	8.15	5.04e-05	6.69	0.00124	0.51
NormOrderedGraphlet-3	10.50	4.33e-05	9.92	0.000135	0.39
NormOrderedGraphlet-3-4	4.31	0.000999	4.92	0.00127	2.41
NormOrderedGraphlet-3-4(K)	<b>1.69</b>	-	<b>2.08</b>	-	2.41
GDDA	17.30	6.16e-09	17.70	2.57e-08	0.54
RGFD	9.46	6.84e-06	9.85	1.39e-05	0.49
GCD	17.10	1.21e-09	17.10	1.51e-08	1.32
GR-align	8.31	0.00705	9.69	0.00423	9.49
Average degree	18.90	2.32e-10	16.20	2.02e-07	0.39
Average distance	15.40	9.54e-07	16.50	3.59e-06	0.48
Maximum distance	17.30	1.58e-09	16.90	4.95e-08	0.49
Average closeness centrality	18.50	2.18e-08	16.50	3.08e-07	0.48
Average clustering coefficient	16.80	5.01e-08	14.50	3.55e-07	0.56
Intra-hub connectivity	16.40	2.84e-08	15.10	1.14e-06	0.64
Assortativity	20.10	1.79e-08	19.20	1.48e-07	0.46
Existing-all	10.90	1.33e-06	10.00	3.05e-05	1.01
DaliLite	12.70	3.27e-05	10.60	0.00192	2021.41
TM-align	22.00	1.85e-12	22.30	5.75e-12	168.32
Sequence	14.50	1.44e-06	16.60	2.1e-08	0.24

**Table 4.** Summary of method accuracy and running times. Accuracy of the given approach is shown with respect to its average ranking compared to all considered approaches across all considered real-world PSN sets, and the results are shown based on AUPR as well as AUROC. The ranking of each method is expressed as follows. For the given PSN set, we determine which approach results in the highest accuracy (rank 1), the second highest accuracy (rank 2), etc. Then, we average the rankings of the given method over all PSN sets. So, the lower the average rank, the better the method. Since NormOrderedGraphlet-3-4(K) has the best average rank with respect to both AUPR and AUROC (shown in bold), we compute the statistical significance of the improvement of NormOrderedGraphlet-3-4(K) over each of the other approaches in terms of their ranks, using paired *t*-test. Running times of the approaches are shown when comparing proteins from the CATH- $\alpha$  set. Running times for the other data sets are qualitatively the same. For visual representation of the results, see Supplementary Fig. S1 and S2.

thus upon the existing methods (Table 3 and Supplementary Table S3). By imposing sequence order onto nodes via ordered graphlets, we further improve the accuracy. By distinguishing between shorter- and longer-range amino acid interactions via “long-range(*K*)” ordered graphlets, we further improve the performance. NormOrderedGraphlet-3-4(K) is superior to all considered methods in terms of its accuracy ranking over all considered PSN sets, and its ranking is statistically significantly better than the ranking of any other method (Table 4). This further validates our graphlet PCA framework for PC.

### 3.3 Application of graphlet PCA measures in revealing biochemically interesting PSN patterns

We aim to identify graphlet patterns that lead to successful distinction of different CATH or SCOP label categories from the PSN data, focusing as an illustration on the PSN sets containing networks of the same size (i.e., on CATH-95, CATH-99, and CATH-251-265) from  $\alpha$  or  $\beta$  protein domain labels. Such graphlets that are significantly (Mann-Whitney U test;  $p < 0.05$ ) represented in  $\alpha$  but not in  $\beta$ , or vice versa, could be linked to the functionality of the given domain label.

For the 3-5-node regular graphlet measure (i.e., Graphlet-3-5), graphlets represented in  $\alpha$  tend to be denser than those represented in  $\beta$  (Fig. 4). For example, all of the complete graphlets (i.e.,  $G_2, G_8, G_{29}$ , which are the densest graphlets) are represented in  $\alpha$ , while all of the path-like graphlets (i.e.,  $G_1, G_3, G_9$ , which are the sparsest graphlets) are represented in  $\beta$ .

For the 3-4-node ordered graphlet measure (i.e., OrderedGraphlet-3-4), in ordered graphlets represented in  $\alpha$  (e.g.,  $O_1$ ), there is typically a node order-respecting path through the graphlet, unlike in most of ordered graphlets represented in  $\beta$  (e.g.,  $O_2$  and  $O_3$ ) (Supplementary Fig. S3). Note that for the data sets from this section (CATH-95, CATH-99, and CATH-251-265), the “long-range(*K*)” constraint does not improve accuracy, and so we do not consider NormOrderedGraphlet-3-4(K) here.

Linking the identified domain label-specific PSN patterns to their potential biochemical meaning is our future interest.

## 4 Conclusions

We present a general computational framework for network comparison, which can use any measure(s) of network topology. We demonstrate the effectiveness of our framework in the context of PC, in particular the power of using graphlets as state-of-the-art network measures. Specifically, we use ordered graphlets to integrate via network analysis complementary protein 3D structural data and sequence data, which improves upon the existing network (graphlet or non-graphlet), 3D contact, and sequence approaches. In the process, we address the network size bias of the existing approaches.

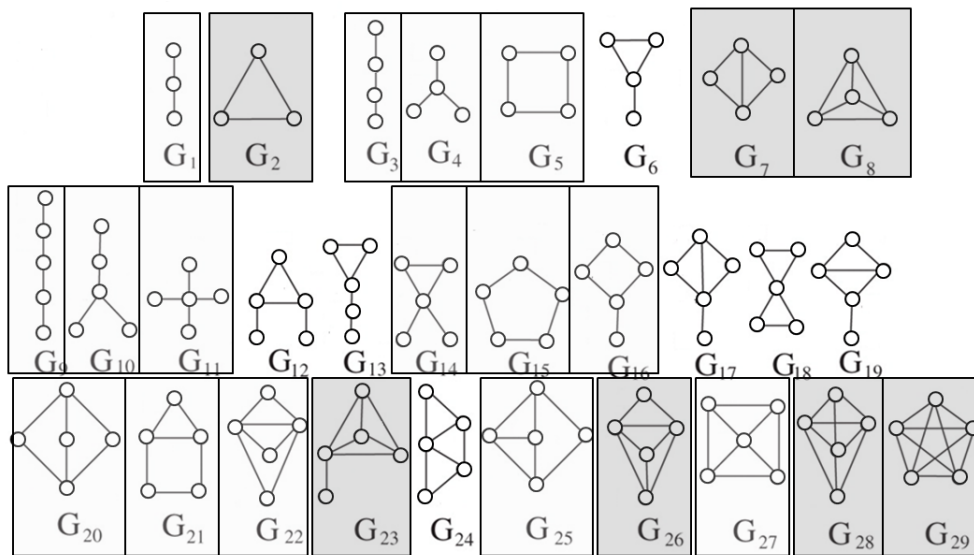


**Figure 4.** Regular (non-ordered) graphlets that are significantly represented in  $\alpha$  (dark gray) or  $\beta$  (light gray) PSNs. For equivalent results for ordered graphlets, see Supplementary Fig. S3.

## References

1. Ashburner, M. *et al.* Gene ontology: tool for the unification of biology. *Nature Genetics* **25**, 25–29 (2000).
2. Kasabov, N. K. *Springer Handbook of Bio-/Neuro-Informatics* (Springer, 2013), 1 edn.
3. Lee, D., Redfern, O. & Orengo, C. Predicting protein function from sequence and structure. *Nature Reviews Molecular Cell Biology* **8**, 995–1005 (2007).
4. Mizianty, M. J. *et al.* Improved sequence-based prediction of disordered regions with multilayer fusion of multiple information sources. *Bioinformatics* **26**, i489–i496 (2010).
5. Sułkowska, J. I., Morcos, F., Weigt, M., Hwa, T. & Onuchic, J. N. Genomics-aided structure prediction. *Proceedings of the National Academy of Sciences* **109**, 10340–45 (2012).
6. Kihara, D. The effect of long-range interactions on the secondary structure formation of proteins. *Protein science : a publication of the Protein Society* **14**, 1955–63 (2005).
7. Krissinel, E. On the relationship between sequence and structure similarities in proteomics. *Bioinformatics* **23**, 717–723 (2006).
8. Gao, J. & Li, Z. Conserved network properties of helical membrane protein structures and its implication for improving membrane protein homology modeling at the twilight zone. *Journal of Computer-Aided Molecular Design* **23**, 755–763 (2009).
9. Tuinstra, R. L. *et al.* Interconversion between two unrelated protein folds in the lyphotactin native state. *Proceedings of the National Academy of Sciences* **105**, 5057–62 (2008).
10. Kosloff, M. & Kolodny, R. Sequence-similar, structure-dissimilar protein pairs in the PDB. *Proteins* **71**, 891–902 (2008).
11. Clarke, T. F. & Clark, P. L. Rare codons cluster. *PLoS One* **3**, e3412 (2008).
12. Burmann, B. M. *et al.* An  $\alpha$  helix to  $\beta$  barrel domain switch transforms the transcription factor RfaH into a translation factor. *Cell* **150**, 291–303 (2012).
13. Holm, L. & Rosenström, P. Dali server: conservation mapping in 3D. *Nucleic Acids Research* **38**, W545–W549 (2010).
14. Zhang, Y. & Skolnick, J. TM-align: a protein structure alignment algorithm based on the TM-score. *Nucleic Acids Research* **33**, 2302–09 (2005).
15. Milenković, T., Filippis, I., Lappe, M. & Pržulj, N. Optimized null model for protein structure networks. *PLoS ONE* **4**, e5967 (2009).
16. Malod-Dognin, N. & Pržulj, N. GR-Align: fast and flexible alignment of protein 3D structures using graphlet degree similarity. *Bioinformatics* **30**, 1259–65 (2014).



17. Emerson, I. A. & Gothandam, K. M. Residue centrality in alpha helical polytopic transmembrane protein structures. *Journal of Theoretical Biology* **309**, 78–87 (2013).
18. Pabuwal, V. & Li, Z. Network pattern of residue packing in helical membrane proteins and its application in membrane protein structure prediction. *Protein Engineering, Design and Selection* **21**, 55–64 (2008).
19. Pabuwal, V. & Li, Z. Comparative analysis of the packing topology of structurally important residues in helical membrane and soluble proteins. *Protein Engineering, Design and Selection* **22**, 67–73 (2009).
20. Emerson, I. A. & Gothandam, K. M. Network analysis of transmembrane protein structures. *Physica A* **391**, 905–916 (2012).
21. Milenković, T., Lai, J. & Pržulj, N. GraphCrunch: a tool for large network analyses. *BMC Bioinformatics* **9** (2008).
22. Memisević, V., Milenković, T. & Pržulj, N. An integrative approach to modeling biological networks. *Journal of Integrative Bioinformatics* **7**, 120 (2010).
23. Kuchaiev, O., Stevanović, A., Hayes, W. & Pržulj, N. GraphCrunch 2: Software tool for network modeling, alignment and clustering. *BMC Bioinformatics* **12** (2011).
24. Faisal, F. E. & Milenković, T. Dynamic networks reveal key players in aging. *Bioinformatics* **30**, 1721–1729 (2014).
25. Pržulj, N., Corneil, D. G. & Jurisica, I. Modeling interactome: Scale-free or geometric? *Bioinformatics* **20**, 3508–3515 (2004).
26. Pržulj, N. Biological network comparison using graphlet degree distribution. *Bioinformatics* **23**, e177–e183 (2007).
27. Hulovatyy, Y., Solava, R. & Milenković, T. Revealing missing parts of the interactome via link prediction. *PLOS ONE* **9**, e90073 (2014).
28. Hulovatyy, Y., Chen, H. & Milenković, T. Exploring the structure and function of temporal networks with dynamic graphlets. *Bioinformatics* **31**, i171–i180 (2015).
29. Solava, R., Michaels, R. & Milenković, T. Graphlet-based edge clustering reveals pathogen-interacting proteins. *Bioinformatics* **18**, i480–i486 (2012).
30. Gromiha, M. M. & Selvaraj, S. Inter-residue interactions in protein folding and stability. *Progress in Biophysics and Molecular Biology* **86**, 235–277 (2004).
31. Berman, H. M. *et al.* The Protein Data Bank. *Nucleic Acids Research* **28**, 235–242 (2000).
32. Sillitoe, I. *et al.* CATH: comprehensive structural and functional annotations for genome sequences. *Nucleic Acids Research* **43**, D376–D381 (2015).
33. Orengo, C. A. *et al.* The CATH database provides insights into protein structure/function relationships. *Nucleic Acids Research* **27**, 275–279 (1999).
34. Murzin, A. G., Brenner, S. E., Hubbard, T. & Chothia, C. SCOP: a structural classification of proteins database for the investigation of sequences and structures. *Journal of Molecular Biology* **247**, 536–540 (1995).
35. Yuan, C., Chen, H. & Kihara, D. Effective inter-residue contact definitions for accurate protein fold recognition. *BMC Bioinformatics* **13**, 292 (2012).
36. Yaveroglu, O. N., Milenković, T. & Pržulj, N. Proper evaluation of alignment-free network comparison methods. *Bioinformatics* **31**, 2697–2704 (2015).
37. Milenković, T. & Pržulj, N. Uncovering biological network function via graphlet degree signatures. *Cancer Informatics* **6**, 257–273 (2008).
38. Milenković, T., Memišević, V., Bonato, A. & Pržulj, N. Dominating biological networks. *PLoS ONE* **6**, e23016 (2011).
39. Aggarwal, C. C. *Data Mining: The Textbook* (Springer, 2015).
40. Yaveroglu, O. N. *et al.* Revealing the Hidden Language of Complex Networks. *Scientific Reports* **4**, 4547 (2014).
41. Vacic, V., Iakoucheva, L. M., Lonardi, S. & Radivojac, P. Graphlet Kernels for Prediction of Functional Residues in Protein Structures. *Journal of Computational Biology* **17**, 55–72 (2010).
42. Lugo-Martinez, J. & Radivojac, P. Generalized graphlet kernels for probabilistic inference in sparse graphs. *Network Science* **2**, 254–276 (2014).

## **Acknowledgements**

This work was supported by the National Science Foundation (CAREER CCF-1452795 and CCF-1319469), Air Force Office of Scientific Research (Young Investigator Program (YIP) FA9550-16-1-0147), National Institutes of Health (1R01GM120733-01A1, 1R21AI111286-01A1, and R01 GM074807), and Clare Boothe Luce Graduate Research Fellowship.

## **Author contributions statement**

F.E.F., J.L.C., P.L.C., and T.M. designed the study. F.E.F. implemented all of the proposed methodology and carried out all of the experiments, with the following exceptions: K.N. implemented the “long-range( $K$ )” approach within the proposed methodology and performed all experiments related to this approach, and J.L. suggested the use of PCA within the proposed methodology. J.L.C. assembled the protein structure datasets. F.E.F., K.N., J.L., S.J.E., P.L.C. and T.M. analyzed the results. F.E.F., J.L.C. K.N., P.L.C., and T.M. wrote the manuscript. All the authors read and approved the manuscript. P.L.C. supervised all applied aspects of the study. T.M. supervised all computational aspects of the study.

## **Additional information**

**Competing financial interests:** The authors declare no competing financial interests.